International Journal of Advanced Research in Engineering and Technology (IJARET)
Volume 11, Issue 12, December 2020, pp. 638-648, Article ID: IJARET_11_12_067
Available online at http://www.iaeme.com/ijaret/issues.asp?JType=IJARET&VType=11&IType=12
ISSN Print: 0976-6480 and ISSN Online: 0976-6499
DOI: 10.34218/IJARET.11.12.2020.067

SOUND ABSORPTION COEFFICIENT OF MPP WITH IRREGULAR HOLES DISTRIBUTION

Al-Ameri Esraa
Fakulti Kejuruteraan Mekanikal, Universiti Teknikal Malaysia Melaka,
Hang Tuah Jaya, 76100 Durian Tunggal, Melaka, Malaysia
State Company of Textile and Leather Industries, Karada - Baghdad, Iraq

A. Putra*
Centre for Advanced Research on Energy, Universiti Teknikal Malaysia Melaka,
Hang Tuah Jaya, 76100 Durian Tunggal, Melaka, Malaysia

R. M. Dan
Fakulti Kejuruteraan Mekanikal, Universiti Teknikal Malaysia Melaka,
Hang Tuah Jaya, 76100 Durian Tunggal, Melaka, Malaysia
Centre for Advanced Research on Energy, Universiti Teknikal Malaysia Melaka,
Hang Tuah Jaya, 76100 Durian Tunggal, Melaka, Malaysia

Ali I. Mosa
Fakulti Kejuruteraan Mekanikal, Universiti Teknikal Malaysia Melaka,
Hang Tuah Jaya, 76100 Durian Tunggal, Melaka, Malaysia
Mechanical Engineering Department, College of Engineering, University of Baghdad,
* Corresponding Author

ABSTRACT

Analytical models for the sound absorption coefficient of MPP are extensively available particularly for the cases where holes are regularly distributed across the MPP structure. The behaviors of sound absorption performance have therefore been well recognized. Thus, it's also interesting to study the MPP for the cases where the distribution of holes is not spaced regularly across the MPP, which becomes the objective of this paper. Here, the FEM is employed to simulate the acoustic impedance of the panel holes. Two main cases of irregular hole distributions are observed, namely 1) where the holes are concentrated in the middle of the plate, and 2) where the holes are distributed around the edge. For each case, this is applied for MPP with homogenous and inhomogeneous perforations. The analysis reveals that for both cases of hole distributions, the peak absorption can shift to lower frequency with the second case to have more effect than the first case. The finite element models are validated with experiment with good agreement.

Keywords: Sound absorption coefficient, MPP, Irregular MPP, Inhomogeneous MPP, FEM.

Cite this Article: Al-Ameri Esraa, A. Putra, R. M. Dan, Ali I. Mosa, Sound Absorption Coefficient of MPP with Irregular Holes Distribution. *International Journal of Advanced Research in Engineering and Technology*, 11(12), 2020, pp. 638-648.
http://www.iaeme.com/IJARET/issues.asp?JType=IJARET&VType=11&IType=12

1. INTRODUCTION

Microperforated panel (MPP) is a thin panel consists of a mesh of sub millimeter size holes circulated through its surface. Its construction is simple and its aesthetic appearance enhances interior design [1], [2]. Not only for building acoustics, but the application can also be extended to acoustic silencers [3], ducted ventilation [4]. MPP acoustic impedance for uniform holes distribution can be easily computed using the analytical method from Maa's equation [1]. When the holes are not regularly distributed, the impedance needs a correction factor which accounts the effect of additional fictitious air mass from neighboring holes, as demonstrated in Ref. [5]. Calculation of acoustic impedance for the irregular hole distribution can be solved numerically for each individual hole by using finite element method to calculate the mechanism of absorption inside the hole [6]–[9]. Carbajo et al. [9] presented the case where the holes in the MPP are shifted closer together while maintaining the perforation ratio, and where the holes are concentrated towards the middle of the panel. It is found that the closer the holes to each other, the more the resonant peak of the absorption coefficient shift to the lower frequency. This paper considering the hole distribution towards the edge of the panel, and also including the case of MPP with inhomogeneous perforation [13]. Experimental results are used to validate the numerical model.

2. BASIC THEORY

2.1. Acoustic Impedance of MPP

The basic structure of a MPP absorber has been first presented by Maa [1]. It comprises of a thin panel containing a set of small holes (less than 1 mm) and backed with air cavity of depth. The acoustic impedance of the MPP contains a resistive-part and a reactive-part. The specific acoustic impedance of a SL- MPP at frequency range is given by [1]

$$Z_{\mathrm{MPP}} = Z_{\mathrm{resistive}} + Z_{\mathrm{reactive}} = r + j\omega m \tag{1}$$

where

$$r = \frac{32\eta t}{\rho c p^2}\left(\sqrt{1+\frac{x^2}{32}} + \frac{xd\sqrt{2}}{8t}\right) \tag{2}$$

$$m = \frac{t}{\rho c}\left[1 + \left(9 + \frac{x^2}{2}\right)^{-1/2} + \frac{0.85d}{t}\right] \tag{3}$$

with p is perforation ratio, t is the thickness of the panel, d is the hole diameter, $x = (d/2)\sqrt{\omega\rho/\eta}$ where ρ is the ambient air density and c is the speed of the sound, $\eta = 1.84 \times 10^{-5}$ is the kinematic viscosity of air, $j = \sqrt{-1}$. The specific acoustic impedance of the rigid back air cavity with depth of (D) is given by [1]

$$Z_D = -j\cot\left(\frac{\omega D}{c}\right) \tag{4}$$

The total acoustic impedance of the MPP system can be represented by an equivalent-electrical-circuit model (ECM) can be written as follows:

$$Z_{\text{total}} = Z_{\text{MPP}} + Z_D \quad (5)$$

2.2. Acoustic Impedance of MPP with inhomogeneous Perforation

Figure 1 (a and b) shows the similar SL-MPP model, but now with an inhomogeneous hole size and ratio. The panel is divided into two-areas (sub-MPP), where each sub-MPP has a different hole diameter and ratio to construct a model of an inhomogeneous MPP. The panel is backed by a rigid wall separated by a uniform air cavity depth. The ECM is shown in Figure 1c.

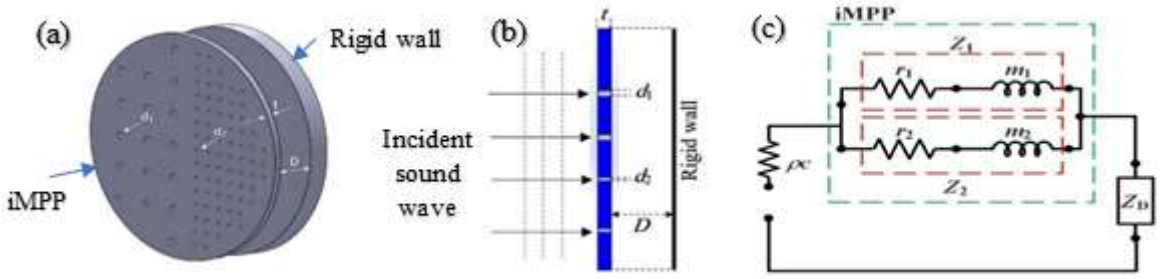

Figure 1 Diagram of an inhomogeneous MPP (iMPP)

The acoustic impedance of the iMPP can be calculated using in Eq. (1). As the two sub-MPPs form a parallel arrangement, thus the specific-acoustic impedance of the iMPP is given as the summation of the two impedance [10] [11]. The iMPP and the back-air cavity are series in the arrangement and thus the total specific-acoustic impedance of the system is:

$$Z_{\text{tot}} = Z_{\text{iMPP}} + Z_D \quad (6)$$

where Z_D the impedance of the air cavity given in Eq. (4). For both Eq. (5) and Eq. (6) the normal incident sound absorption coefficient of the MPP system can be calculated by:

$$\alpha = \frac{4\text{Re}\{Z_{\text{tot}}\}}{[1+\text{Re}\{Z_{\text{tot}}\}]^2+[\text{Imag}\{Z_{\text{tot}}\}]^2} \quad (7)$$

The acoustic impedance model in Eqs. (1)-(3) proposed by Maa [1] assumes a uniform distribution of holes. As discussed in [9], when the spatial distribution is no longer uniform, the model is also no longer valid as it ignores the interaction between holes, especially as the holes become closer together in a group. The phenomenon has also been discussed in [5]. The (FE) model is therefore proposed in [9] to be able to simulate the effect of fluid-hole interaction at the vicinity of the hole edge. Similar FE model is applied here for the case of holes concentrated in the center and through the edge of the MPP and also for MPP with inhomogeneous perforation.

3. FINITE ELEMENT MODEL

3.1. Model Setup

Numerical simulation using FE model in COMSOL Multiphysics is conducted to study the acoustic performance of SL-MPP with homogeneous and inhomogeneous perforation and with regular and irregular holes distribution. The method employs the linearized Naiver-Stokes equations. Figure 2 shows the schematic diagram of the assumed symmetry boundaries of an iMPP sample. To save the computational time, the MPP can be divided into two equal areas across the sub-MPPs, so that the half-area contains half of the sub-MPP. It should be

noted that for homogenous MPP, it is sufficient to model only a quarter area of the MPP to speed up the numerical calculation.

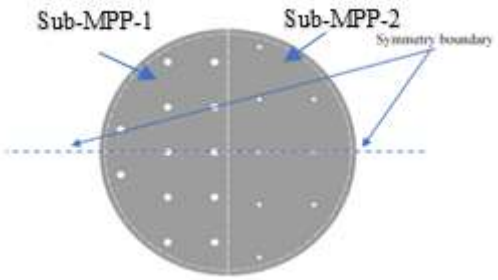

Figure 2. The schematic graph shows a front view of the iMPP sample with the assumed symmetry boundaries

Figure 3 shows the construction of the 3D structure in the FE model that combines the iMPP inside a cylindrical tube in front of an air cavity and also back by an air cavity with rigid termination. The tube has a thickness of 1 mm, with a length of 300 mm and an inner diameter of 33 mm. An adiabatic plane acoustic wave field is generated by a sound source located at the front boundary to excite the MPP. The tube walls, the iMPP and the backed wall are assumed to be acoustically rigid (no vibration) and isothermal

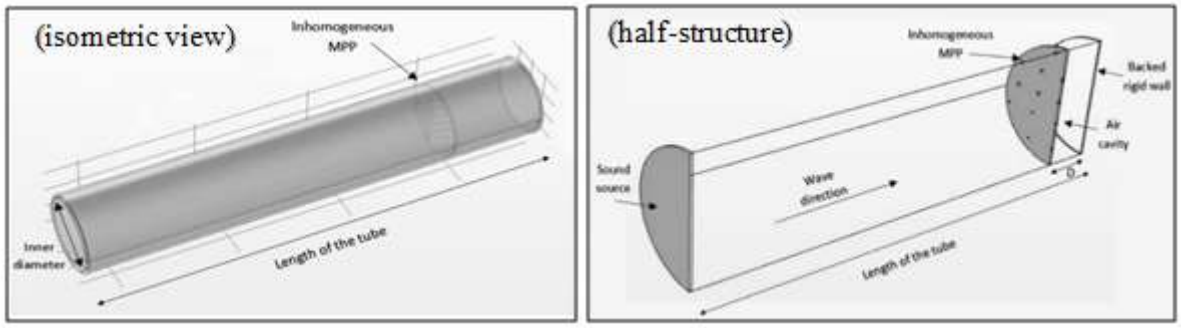

Figure 3 Schematic diagram of the 3D-FE model for the impedance tube with the iMPP

The specific acoustic impedance of the MPP in the FE model can be obtained by calculating the ratio of the pressure gradient across the panel to the velocity of the fluid across the hole in the direction of propagation. This can be represented by [6]

$$Z_{\text{MPP}} = \frac{\int P_i - \int P_t}{\rho c \int v} \tag{8}$$

where P_i represents the total incident sound pressure at the front surface of the MPP and P_t is the total transmitted sound pressure at the back surface of the MPP, and v is the average particle velocity of the fluid. The total impedance of the model is then can be calculated using Eq. (5) or Eq. (9).

3.2. Mesh Setup

The implementation of the size of the mesh elements in the FE model is first studied to ensure the model produces valid results of acoustic impedance up to the maximum frequency of interest. Following the method in [9], here the unstructured Tetrahedral Taylor–Hood-like mesh element is applied to the FE model. Figure 4 depicts the 3D view of the mesh in the FE model.

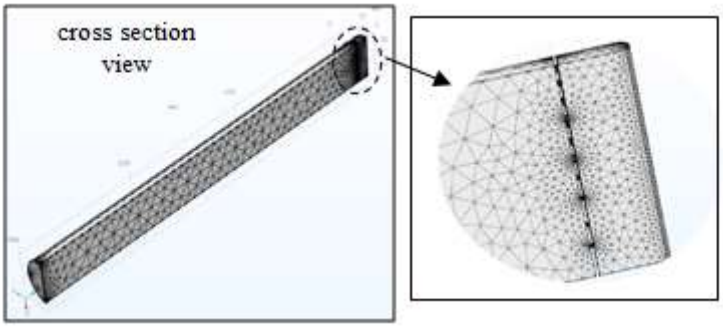

Figure 4 Mesh implementation for the 3D impedance tube including the iMPP sample

Four different sizes of mesh elements are selected to conduct the convergence test as listed in Table 1. The custom mesh element size is set to give a greater degree of freedom compared to that of the finer one. Figure 5 shows the simulated acoustic impedance real and imaginary parts for each mesh size. It can be seen that the finer mesh with the greatest number of degrees-of-freedom has the same result with that of the custom mesh with a negligible difference. The finer mesh is therefore chosen to calculate the absorption coefficient of the MPP system.

Table 1 Mesh element characterization in the FEM

Cases	Type of Mesh	Domain-elements	Boundary-elements	Edge-elements	degrees of freedom
Mesh-1	Normal	19033	7208	757	127881
Mesh-2	Fine	36862	11784	1083	241167
Mesh-3	Finer	83981	19765	1460	529109
Mesh-4	Custom	84545	20604	1519	677677

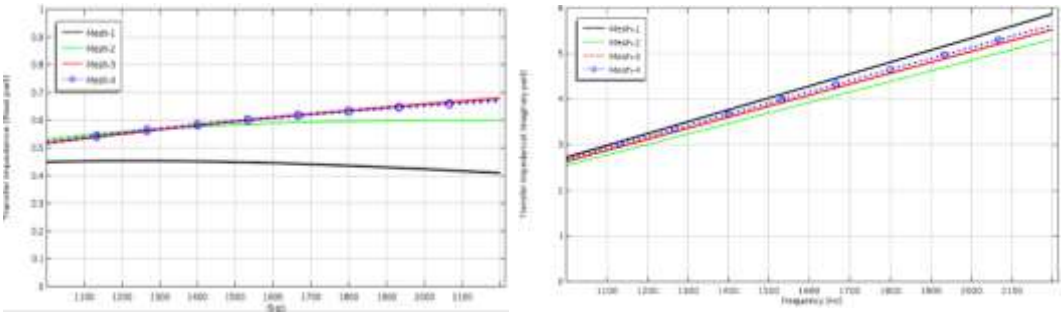

Figure 5 Acoustic impedance real and imaginary parts for different sizes of mesh element

4. SIMULATION RESULTS

4.1. Validation of FEM with ECM

In this section, validation of the simulation results from the FEM with the ECM is to ensure the FEM has a correct assumption of boundary conditions and size of the mesh. Firstly, simulation of the absorption coefficient of MPP with homogenous perforation is presented as listed in Table 2 and shown in Figure 6. The results in Figure 7 show a good agreement between both methods.

Table 2 Structural parameters of MPP samples with homogeneous perforation

Sample	Sample diameter, (mm)	Panel thickness, t (mm)	Hole-diameter, d (mm)	Perforation-ratio, p (%)
MPP – 1	33	1	0.5	0.67
MPP – 2	33	1	0.7	0.95
MPP – 3	33	1	0.9	1.70

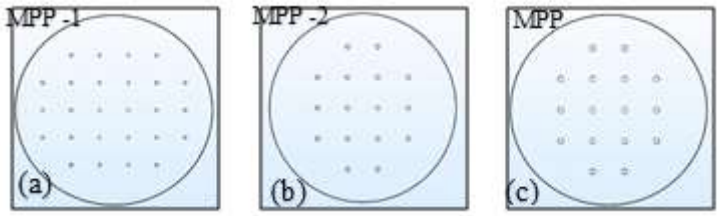

Figure 6 Diagram of the MPPs with homogeneous perforation

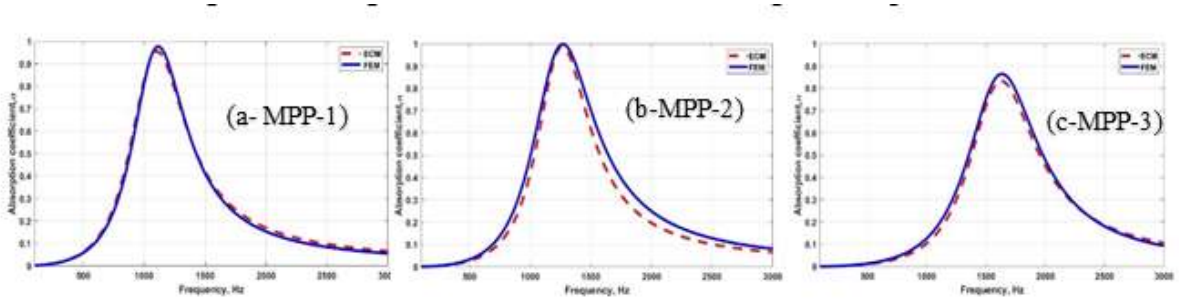

Figure 7 Comparison of the absorption coefficient obtained from ECM and FEM for MPP

Furthermore, Table 3 listed the structural parameters for iMPP as shown in the Figure 8

Table 3 Structural parameters of MPP models with inhomogeneous perforation

Sample	Sample diameter, (mm)	Panel thickness, t (mm)	Sub-iMPP$_1$		Sub-iMPP$_2$	
			Hole Diameter, d_1 (mm)	Perforation ratio, p_1 %	Hole diameter, d_2 (mm)	Perforation ratio, p_2 %
iMPP-1	33	1	0.9	1.76	0.5	0.40
iMPP-2	33	2	0.9	3.97	0.4	1.49
iMPP-3	33	1	0.9	0.60	0.4	3.00

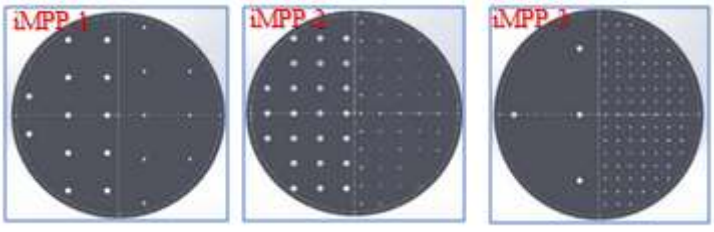

Figure 8 Diagram of MPPs with inhomogeneous perforation

Figure 9 shows the absorption coefficient calculated using the ECM and the FEM. A good agreement can be observed between both methods. For example, in Fig 9(a), the FEM produces a resonant peak at a slightly lower frequency. As the impedance of the cavity depth for both models is calculated using the same equation (Eq. (4)), these differences are mainly due to the finite geometry effect and the spatial distribution of the perforations in the FEM.

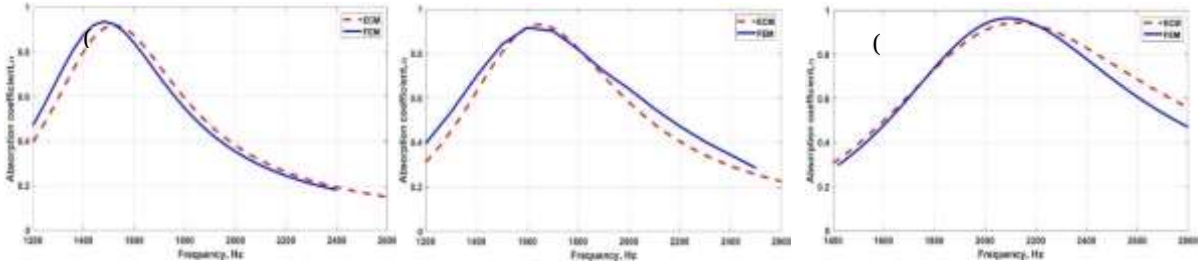

Figure 9 Comparison of the absorption coefficient obtained from ECM and FEM for SL-iMPP, cavity depth D= 10 mm, (a) iMPP-1, (b) iMPP-2, (c) iMPP-3

The following section presents of MPP in the modification the FEM into irregular holes distribution,

4.2. Parametric Study

To simulate the effect of irregularity distribution of holes in MPP on sound absorption performance, three conditions are defined:

- Holes with almost equal spacing (regularly distributed, as the baseline).
- Holes which are concentrated at the center of the MPP.
- Holes which are distributed around the edge of the MPP.

4.2.1. Homogeneous Perforation

Table 4 lists the structural parameters of the homogeneous MPP which perforation. The number at each group defines the following

- Holes with regular distribution
- Holes concentrated in the middle
- Holes distributed at the edge

The diagram is shown in Figure10.

Table 4 Parameters of MPP models with homogeneous perforation

Group	Models	Model diameter, (mm)	*t* (mm)	*d* (mm)	Number of-holes,
A	MPP (A1-A3)	33	1	0.5	6
B	MPP (B1-B3)	33	1	0.5	14
C	MPP (C1-C3)	33	1	0.5	28
D	MPP (D1-D3)	33	1	0.5	56

Figure 11 shows the simulation results of the MPP models groups (A to D). The results demonstrate that for the holes distribution around the edge of the MPP, the peak absorption shifts to lower frequency. Reduced peak and absorption bandwidth can be seen for low perforation ratio, and this improves as the perforation ratio is increased. For the holes in the middle, the peak is also slightly shifted to lower frequency. As shown in [9], the smaller the hole separation, the lower the shifting of the peak frequency. As the holes are closer, the holes have added fictitious mass from neighboring holes and therefore this added mass in turn, reduces the resonant frequency.

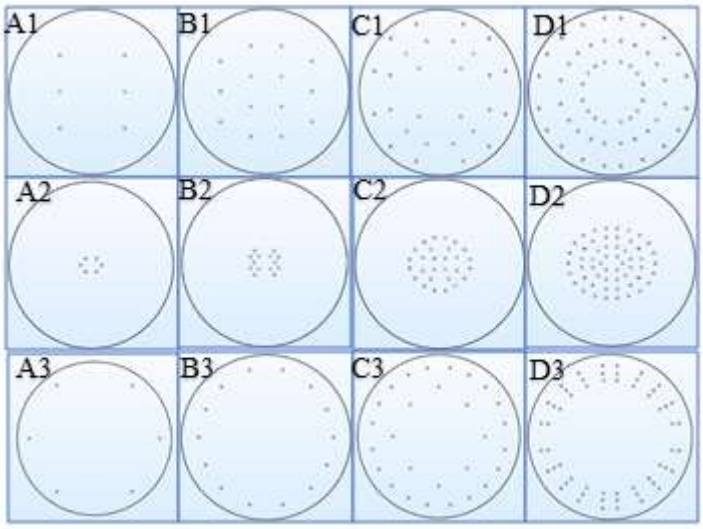

Figure.10 Diagram of MPPs with different spatial distribution of holes, (A1-D1): regularly distributed, (A2 -D2): concentrated in the middle, (A3 -D3): distributed at the edge

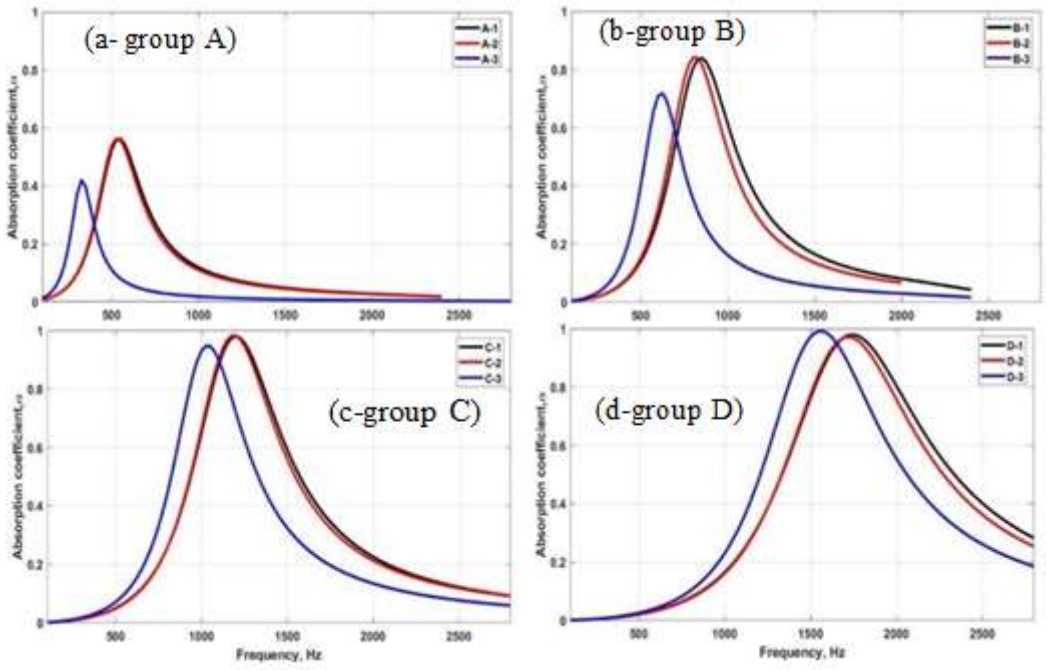

Figure.11. Simulation Results presenting the effect of hole distribution on absorption coefficient

4.2.2. Inhomogeneous Perforation

The simulation for the case of inhomogeneous perforation (iMPP) is to observe whether the phenomenon found in the homogeneous case also hold for the inhomogeneous case. Table 5 lists the structural parameters and the figures of MPP as shown in Figures 12. The models are now divided into the groups: E, F, G, and H. The models are designed where the number of holes is varied from sub-MPP_1 and is fixed for sub-MPP_2.

Table 5 Parameters of inhomogeneous MPP models.

MPP Group	Model	Model diameter, (mm)	Thickness, t (mm)	Sub-MPP$_1$		Sub-MPP$_2$	
				d_1 (mm)	holes number	d_2 (mm)	holes number
E	i-MPP (E1-E3)	33	2	0.8	3	0.5	34
F	i-MPP (F1-F3)	33	2	0.8	7	0.5	34
G	i-MPP (G1-G3)	33	2	0.8	14	0.5	34
H	i-MPP (H1-H3)	33	2	0.8	28	0.5	34

The results of the simulation are in Figure 13 plotted in the frequency range from 1 to 2.8 kHz highlighting the performance around the resonant peak of the sound absorption coefficient. It is demonstrates that for the holes distributed around the edge of the plate, the absorption coefficient can be seen to shift to the lower frequency but with the bandwidth of absorption to remain unchanged compared to the case of regularly distributed holes. This opens the possibility for alternative control of absorption performance and alternative aesthetic design to the conventional MPP with regular hole arrangement.

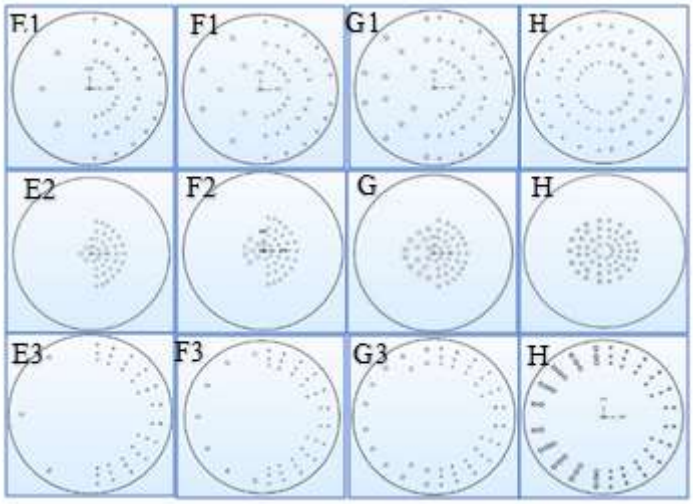

Figure 12 Diagram of iMPP with variation of spatial distribution of holes: column (E1-H1): regularly distributed, (E2-H2): concentrated in the middle, (E3-H3): distributed at the edge

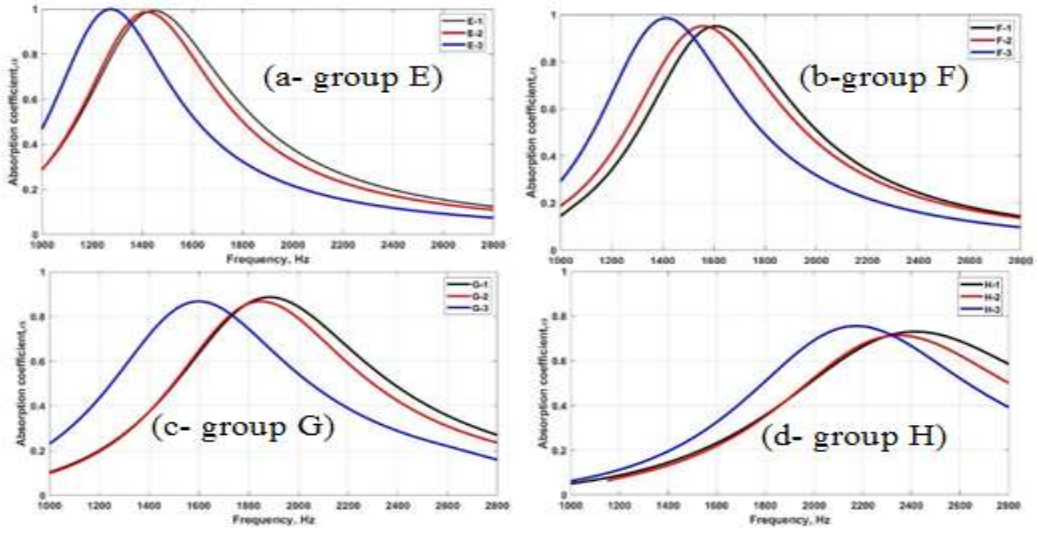

Figure.13 Result of simulation presenting the effect of hole distribution on absorption coefficient for the iMPP

5. EXPERIMENT

The measurement of the normal sound absorption coefficient was carried out by use of the impedance tube apparatus based on the transfer function method according to ISO 10534-2 [12]. The measurement setup is the same as in Ref. [13]. Three samples of inhomogeneous MPPs (as listed in table 6) with different holes distribution where fabricated and the same number of the holes in each panel is 62 as shown in Figure 14.

Table 6 Structural parameters of the MPP samples

Sample	Sample diameter	t (mm)	d_1 (mm)	d_2 (mm)	holes number
iMPP-1	33 mm	1	0.7	0.5	62
iMPP-2	33 mm	1	0.7	0.5	62
iMPP-3	33 mm	1	0.7	0.5	62

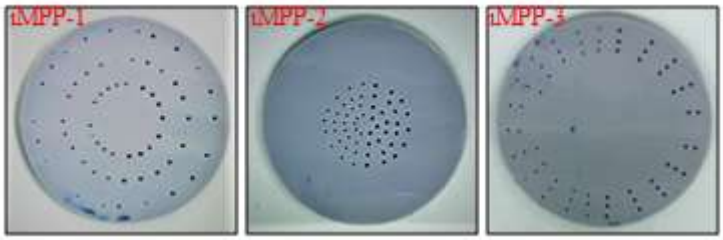

Figure 14 iMPP test samples with different hole distribution.

Figure 15 shows the comparison of the absorption coefficient between the measured data with those obtained from the FEM for a back cavity depth of D = 10 mm. Generally, a good agreement can be observed between the experiment and the FEM. Simulation is achieved that the peak shifted from 2.2 kHz for the case of regularly distributed holes (Fig. 15 (a)) to 2 kHz for the case of holes distributed at the edge (Fig. 15 (c)) can be observed and is validated by the experimental result.

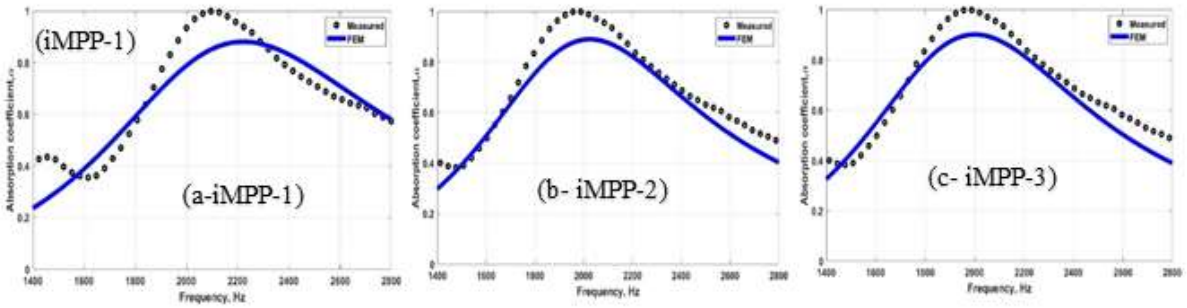

Figure 15 Comparison of the absorption coefficient between the FEM and measured data

6. CONCLUSION

In this paper, a 3D finite element model (FEM) is built to study the acoustic properties of a single-layer MPP absorber with regular and irregular hole distribution. Two types of MPP models, namely homogeneous and inhomogeneous perforation are simulated to analyze the sound absorption coefficient. Simulation results show that the absorption coefficient shifts to lower frequency region for holes concentrated around the edge of the MPP. For the particular

case in this paper, the peak can be 200 Hz lower than for the MPP with a regular distribution of holes. The peak absorption is also shifted slightly to low frequency for the case of holes concentrated in the middle of the MPP. The experiment results have good agreement with the FE models. This opens the possibility for alternative control of absorption performance and alternative aesthetic design to the conventional MPP with regular hole arrangement.

ACKNOWLEDGEMENT

Part of this project is supported by the Fundamental Research Grant Scheme from the Ministry of Higher Education Malaysia No. FRGS/1/2016/ TK03/FTK-CARE/F00323.

REFERENCES

[1] D. Maa, "Theory and Design of Microperforated Panel Sound-Absorbing Constructions," *Scientia Sinica*, vol. 18, no. 1. pp. 55–71, 1975.

[2] A. I. Mosa, A. Putra, R. Ramlan, and A. A. Esraa, "Micro-perforated panel absorber arrangement technique: A review," *J. Adv. Res. Dyn. Control Syst.*, vol. 10, no. 7, pp. 372–381, 2018.

[3] X. Shi and C. M. Mak, "Sound attenuation of a periodic array of micro-perforated tube mufflers," *Appl. Acoust.*, vol. 115, pp. 15–22, 2017.

[4] X. Yu, F. S. Cui, and L. Cheng, "On the acoustic analysis and optimization of ducted ventilation systems using a sub-structuring approach," *J. Acoust. Soc. Am.*, vol. 139, no. 1, pp. 279–289, 2016.

[5] R. Tayong, "Effects of unevenly distributed holes on the perforated plate sound," *Noise Control Eng. J.*, vol. 61, no. December, pp. 547–552, 2013.

[6] L. Li, X. Gang, Y. Liu, X. Zhang, and F. Zhang, "Numerical simulations and experiments on thermal viscous power dissipation of perforated plates," *AIP Adv.*, vol. 8, no. 10, 2018.

[7] J. Carbajo, J. Ramis, L. Godinho, P. Amado-Mendes, and J. Alba, "A finite element model of perforated panel absorbers including viscothermal effects," *Appl. Acoust.*, vol. 90, pp. 1–8, 2015.

[8] W. M. Beltman, P. J. M. Van Der Hoogt, R. M. E. J. Spiering, and H. Tijdeman, "Implementation and experimental validation of a new viscothermal acoustic finite element for acousto-elastic problems," *J. Sound Vib.*, vol. 216, no. 1, pp. 159–185, 1998.

[9] W. R. Kampinga, Y. H. Wijnant, and A. De Boer, "Performance of several viscothermal acoustic finite elements," *Acta Acust. united with Acust.*, vol. 96, no. 1, pp. 115–124, 2010.

[10] I. Prasetiyo, J. Sarwono, and I. Sihar, "Study on inhomogeneous perforation thick micro-perforated panel sound absorbers," *J. Mech. Eng. Sci.*, vol. 10, no. 3, pp. 2350–2362, 2016.

[11] A. I. Mosa, A. Putra, R. Ramlan, I. Prasetiyo, and A.-A. Esraa, "Theoretical model of absorption coefficient of an inhomogeneous MPP absorber with multi-cavity depths," *Appl. Acoust.*, vol. 146, 2019.

[12] International Organization for Standardization, "Acoustics- Determination of Sound Absorption Coefficient and Impedance in Impedance Tubes," *Int. Stand.*, 2001.

[13] A. I. Mosa, A. Putra, R. Ramlan, and A. A. Esraa, "Wideband sound absorption of a double-layer microperforated panel with inhomogeneous perforation," *Appl. Acoust.*, vol. 161, p. 107167, 2020.